Astronomy & Astrophysics manuscript no. master
December 18, 2017

High resolution near-IR spectroscopy of Arcturus and 10 Leo

Refining a near-IR iron line list

D. T. Andreasen[1,2], S. G. Sousa[1], E. Delgado Mena[1], N. C. Santos[1,2], T. Lebzelter[3], A. Mucciarelli[4,5], and J.J. Neal[1,2]

[1] Instituto de Astrofísica e Ciências do Espaço, Universidade do Porto, CAUP, Rua das Estrelas, 4150-762 Porto, Portugal, e-mail: daniel.andreasen@astro.up.pt
[2] Departamento de Física e Astronomia, Faculdade de Ciências, Universidade do Porto, Rua Campo Alegre, 4169-007 Porto, Portugal
[3] Institute for Astrophysics, University of Vienna, Türkenschanzstrasse 17, 1180 Vienna, Austria
[4] Dipartimento di Fisica e Astronomia, Universita' degli Studi di Bologna, Viale Berti Pichat, 6/2, 40126, Bologna, Italy
[5] INAF - Osservatorio Astronomico di Bologna, Via Ranzani 1, 40127, Bologna, Italy

Received ...; accepted ...

ABSTRACT

Context. Reliable stellar atmospheric parameters for FGK stars have been **commonly** obtained from methods that rely on high resolution and high S/N optical spectroscopy. The advent of a new generation of high resolution ($R > 50\,000$) near-IR spectrographs opens the possibility of using classic spectroscopic methods with high resolution and high S/N in the NIR spectral window.
Aims. We aim to **refine a NIR iron line list for determination of stellar atmospheric parameters. For verification we derive parameters of two K giant stars, Arcturus and 10 Leo.**
Methods. Our spectroscopic analysis is based on the iron excitation and ionization balance done in LTE and a line list of Fe I and Fe II lines in the NIR domain. The line list is being refined from our previous study, allowing us to obtain more reliable parameters.
Results. **We present an updated line list for the derivation of stellar parameters in the NIR that has allowed us to successfully** obtain parameters for two K giants in agreement with average literature values adopted.
Conclusions. With these results we are now extending our previous line list towards cooler stars, thus allowing us to explore the M dwarf stars in the future. **The improvement of the derivation of stellar parameters for M dwarfs is very important for the study of the Galactic Chemical Evolution and crucial for the characterisation of Earth-like planets, expected to be very common around these kind of stars.**

Key words. data reduction: high resolution spectra – stars individual: Arcturus – stars individual: 10 Leo

1. Introduction

The stellar atmospheric parameters such as the effective temperature ($T_{\rm eff}$), surface gravity ($\log g$), and metallicity ([M/H], where iron is normally used as a proxy) are fundamental to determine in order to characterise a single star, and to indirectly determine other fundamental parameters such as mass, radius, and age from stellar evolution models (see e.g. Girardi et al. 2000; Dotter et al. 2008; Baraffe et al. 2015). **These parameters are crucial to know with high precision and accuracy when deriving planetary masses and radii of exoplanets which are directly related to its stellar host** (see e.g. Torres et al. 2008; Ammler-von Eiff et al. 2009; Torres et al. 2012).

The derivation of precise stellar atmospheric parameters is not a simple task. Different approaches often lead to discrepant results (see e.g. Torres et al. 2010; Lebzelter et al. 2012a; Santos et al. 2013). Interferometry is usually considered an accurate method for deriving stellar radii (see e.g. Boyajian et al. 2012); however, it is only applicable for bright nearby stars. Asteroseismology **can be used to reveal the inner structure of stars by carefully observing the pulsations of the stellar surface. Oscillations patterns make it possible to derive the surface gravity and mean density, thus allowing calculations of the stellar mass and radius with high precision** (see e.g. Kjeldsen & Bedding 1995, for scaling relation of dwarf stars). **It is important to note that asteroseismology of solar-like oscillations are only applicable for FGK stars. We have yet to detect oscillations in the low-luminosity M stars** (Rodríguez et al. 2016; Berdiñas et al. 2017). Moreover, $T_{\rm eff}$ is needed when applying asteroseismology in order to obtain the surface gravity and the mean density.

A crucial parameter for the indirect determination of stellar bulk properties is $T_{\rm eff}$. In that respect, the infrared flux method (IRFM) has proven to be reliable for FGK dwarf and subgiant stars. For higher accuracy the IRFM needs a priori knowledge of the bolometric flux, reddening, surface gravity, and stellar metallicity (Blackwell & Shallis 1977; Ramírez & Meléndez 2005; Casagrande et al. 2010). Finally, the use of high resolution spectroscopy along with stellar atmospheric models is an extensively tested method that allows the derivation of the fundamental parameters of a star (see e.g. Valenti & Fischer 2005; Santos et al. 2013; Worley et al. 2016). **The procedure depends on the quality of the spectra, their resolution, wavelength region, and the set of software used. The latter includes the atmosphere models, radiative transfer code, and the atomic data used.** A fit to the overall spectrum can be applied for all spectral resolutions, but is often time consuming (see e.g. Recio-Blanco et al. 2006; Tsantaki et al. 2017). For resolutions larger than $\lambda/\Delta\lambda > 50\,000$ we can apply the equivalent width (EW) method (see e.g. Tsantaki et al. 2013; Andreasen et al. 2017, for details). However, while the latter approach is often faster than the synthetic fitting, it requires high quality spectra, and the star

to be a slow rotator (below 10 km/s to 15 km/s). **It also fails for cool stars due to severe continuum depression.**

Standard procedures are often used to derive stellar atmospheric parameters from high quality spectra in the optical (see e.g. Valenti & Fischer 2005; Sousa et al. 2008). With the advancement of high resolution near-infrared (NIR) instruments, that is resolution higher than approximately 50 000, we will now be able to use a similar technique to that used in the optical part of the spectrum (see e.g. Meléndez & Barbuy 1999; Sousa et al. 2008; Tsantaki et al. 2013; Mucciarelli et al. 2013; Bensby et al. 2014; Andreasen et al. 2017). Such an effort seems very timely because of the growing number of observing facilities offering a high-resolution access to the near infrared range. **For a quick description of up-comming/installed high resolution spectrographs see the introduction in** Andreasen et al. (2016) (referred to as Paper I).

With the advance of the next generation **high resolution** NIR spectrographs, we are still preparing the data analysis of stellar spectra, in particular how to get reliable atmospheric parameters (see e.g. Önehag et al. 2012; Lindgren et al. 2016; Andreasen et al. 2016). The analysis of stellar spectra is well understood for FGK stars in the optical part of the spectrum, however some work still needs to be done for the NIR part.

We continue our series of studies to explore the use of the NIR domain to derive stellar parameters for FGK and M stars. Here we analyse the atlas of Arcturus and the spectrum of 10 Leo. For the analysis we use the iron line list presented in Paper I **which is improved and updated in this work**. In Paper I we successfully tested our method on a slightly hotter star than the Sun, while in this work we aim to test the method on cooler stars. The strength of the NIR domain over the optical becomes clear when we move towards the cooler stars. Here we see less continuum depression and line blending due to in particular molecular features **which are more prominent in the optical part for cool stars**. Moreover, the coolest stars emit more light in the NIR domain than the optical, and with the stars with the lowest masses being intrinsically faint, we thus obtain the majority of the flux here.

2. Data

2.1. The stars

While the community is currently on the verge to access large amounts of high resolution NIR spectra, the available spectra at the moment are sparse. We chose to use two stars cooler than the Sun since we used a star hotter than the Sun (the subgiant HD 20010) in Paper I **as it was one of the stars with stellar atmospheric parameters closet to that of the Sun, thus making it a good test at the time**. We will however use all four stars in this work for various reasons. The solar spectrum will be used for inspecting the line list presented in Paper I. This spectrum was obtained from the Kitt Peak telescope by Hinkle et al. (1995b). The spectrum of HD 20010 will be reused from Paper I as well. This spectrum was obtained with the CRIRES spectrograph by Lebzelter et al. (2012b) as part of the CRIRES-POP. HD 20010 will be reanalysed as to confirm the improvement of the refined line list which will be presented in the section below. The two stars which we have not analysed before are Arcturus and 10 Leo. These two extra stars will increase the range of spectral type for the test of the line list, allowing to test cool giant stars with different metallicities regimes.

Arcturus is one of the brightest stars on the Northern hemisphere, and is well studied (see e.g. Griffin & Griffin 1967; McWilliam 1990; Ramírez et al. 2013, to mention just a few), and a benchmark star in current spectroscopic surveys such as Gaia-ESO (Jofré et al. 2014; Smiljanic et al. 2014). The atlas of Arcturus (acquired at Kitt Peak National Observatory using the FTS spectrograph at the Mayall telescope by Hinkle et al. (1995a)), covers the spectral range of interest (YJHK bands). Strong telluric features were identified with a spectrum from the TAPAS web page (Bertaux et al. 2014). The atlas also comes with a telluric standard and the ratio of the two spectra in order to correct for the tellurics. The telluric spectrum from TAPAS is only used for telluric line identification. We use both the telluric corrected and non-corrected spectrum.

The spectrum for 10 Leo is made available by the CRIRES-POP team (Nicholls et al. 2017). 10 Leo is very similar to Arcturus, which is also one reason this star was the first to be fully reduced by the CRIRES-POP team. The spectrum is divided into several pieces according to the atmospheric windows in the NIR: YJ (only together), H, K, L, and M. We use only the first three. Some small gaps are present in the spectrum due to tellurics that could not be properly removed, low S/N, bad pixels, etc. Rather than giving an uncertain interpolation, Nicholls et al. (2017) decided to leave small gaps in the data. This has very little effect on our line by line analysis, however, due to those gaps, we were unable to measure one Fe II line which are generally important to determine the surface gravity.

The data for the two stars are very similar in terms of S/N (around 300 as measured by IRAF in a continuum region in the YJ band), resolution (approximately 100 000), and spectral coverage.

A summary of the four stars used can be seen in Table 1. The parameters are obtained from the PASTEL catalogue (Soubiran et al. 2016) which is a compilation of stellar atmospheric parameters from the literature obtained mostly from high resolution and high S/N spectra. **Specifically for Arcturus, we use the same parameters as reported in Table 1 in** Jofré et al. (2014). **These parameters are a mean from the PASTEL catalogue between 2000 and 2012.** The parameters are the median values of all measurements for a given star, where the errors reported are the standard deviation of those values. $\xi_{\rm micro}$ is estimated using the empirical relation by Tsantaki et al. (2013) for **HD 20010**, and Adibekyan et al. (2015) for the **10 Leo. For Arcturus the value is a mean of the derived microturbulence from different groups as explained in** Jofré et al. (2014). This is done for each literature value in the catalogue. The value presented in the Table here is calculated on the same way as the rest of the parameters.

2.2. The line list

There have been different recent studies compiling line lists for high resolution NIR spectra. For M dwarfs there is the line list by Önehag et al. (2012); Lindgren et al. (2016), which has been tested extensively on CRIRES spectra ($R \sim 100\,000$) using the spectral synthesis method.

Since we wanted to compile a line list for FGK, and possible M dwarf stars, suitable for the EW method, we decided to start from the VALD3 database (Piskunov et al. 1995; Kupka et al. 2000). This has not been done for the NIR previously. In Paper I we prepared a Fe I and Fe II line list in the NIR domain. The atomic data from the lines were in a wavelength region ranging from (10 000 to 25 000) Å, covering the YJHK bands. EWs were measured for all iron lines with ARES (Sousa et al. 2015), discarding any line with EW below 5 mÅ or above 200 mÅ. The

Table 1. Summary of the four stars used in this work. The stellar parameters are from the PASTEL catalogue (Soubiran et al. 2016) (see text for details), except the parameters for the Sun.

Star	Spectrographs	Resolution	$T_{\rm eff}$ (K)	$\log g$ (dex)	$\xi_{\rm micro}$ (km/s)	[Fe/H] (dex)
Sun	FTS	600 000	5777	4.44	1.00	0.00
Arcturus	FTS	100 000	4247 ± 37	1.59 ± 0.04	1.30 ± 0.12	−0.54 ± 0.04
HD 20010	CRIRES	100 000	6152 ± 95	3.96 ± 0.11	1.17 ± 0.24	−0.27 ± 0.06
10 Leo	CRIRES	100 000	4742 ± 61	2.76 ± 0.17	1.45 ± 0.08	−0.03 ± 0.02

oscillator strengths of the line list was calibrated using the solar spectrum, and the solar iron abundance from Gonzalez & Laws (2000) at 7.47 dex **which is used in our group as a reference.**. The abundances of individual iron lines were obtained with the radiative transfer code MOOG (Sneden 1973) assuming LTE and using ATLAS model atmospheres (Kurucz 1993). The line list was successfully used to derive atmospheric parameters for a late F star, HD20010.

3. Refining the NIR line list

In this work we will go one step forward, and test the previous line list for two K type stars. Before testing the line list from Paper I at cooler effective temperatures with two K stars, it is a primary goal of this work to refine the line list. This includes identifying recurring outliers (both from the work done in Paper I and in this work), and lines which we are not able to measure, e.g. if a line is amidst a forest of telluric lines. The refinement is needed, since we experienced **an over-estimated metallicity of around 0.1 dex for HD 20010 compared to the literature value used in Paper I.** The errors on all parameters were also quite high compared to what is achievable for similar quality spectra from the visible. To identify these lines the solar atlas used in Paper I was revisited. In total 211 out of 295 Fe I lines and 8 out of 13 Fe II lines were removed in the process. Most of these were blended lines with either tellurics or other stellar lines. This procedure leaves us with 84 Fe I lines and 5 Fe II lines. These lines should be the best for deploying our technique of determining atmospheric stellar parameters.

During a second look at the Solar spectrum, the EW of the lines were measured by hand (this had previously been done automatically with ARES). Since we re-measured the EWs, the oscillator strengths, $\log gf$, had to be re-calibrated again. Here we simply change the $\log gf$ values for the measured EW until the abundance of a given line is equal to that of the Sun, using the same solar atmosphere model as in Paper I. The mean change in $\log gf$ for common lines is -0.09 ± 0.16. The line list with the updated $\log gf$ is presented in Table A.1.

The Fe II lines are used to determine $\log g$ by imposing ionization balance with the average Fe I abundance. However, the low number of Fe II lines available is a concern, since the average abundance of Fe II is affected more by small number statistics compared to the numerous Fe I lines.

4. Obtaining stellar parameters

The method used both in Paper I and here is based on the determination of the iron abundances on a number of lines from their measured EWs. This is done using the radiative transfer code MOOG (Sneden 1973) to determine the iron abundance from the measured EWs. Then, ionization balance between Fe I and Fe II lines, and excitation balance for all Fe I lines is imposed, by changing the atmospheric parameters for the model atmosphere (Kurucz 1993, ATLAS9 is used here). While this is a well tested method for getting atmospheric parameters utilising the optical part of the spectrum, **little work have been done with the EW method in the NIR domain. Therefore we approach the measurements of the EWs with extra care, thus** the measurements of EWs are done with both manually (IRAF) and automatically (ARES) as a quality check. For both the automatically and manually measured EWs, we discard all lines with an EW below 5 mÅ and above 150 mÅ before continuing the analysis. We decided to be a bit more constrained in the upper limit for the line strength decreasing it to 150 mÅ to be sure that the Gaussian fit is a good approximation. Lines outside this range are either too weak to be reliably measured or saturated and do no longer contain information about the abundance. The entire procedure of obtaining the stellar parameters is done with the software FASMA (Andreasen et al. 2017) which does the minimization when imposing ionization end excitation balance.

5. Results

The results for the revisited spectrum of HD 20010, and the two additional K stars are presented here. We do not present the results for the Sun since the line list is calibrated for this star[1].

5.1. Revisiting HD 20010

As a first step we revisit HD 20010 for which we derived atmospheric stellar parameters in Paper I using the newly revised line list presented in this paper. The results are shown in Table 2 along with the **results for the two other stars analysed in this work**. We see better agreement with the average literature values adopted (especially [Fe/H] and $\log g$), and smaller errors with the updated results. This suggests that the new line list is more reliable.

The parameters for the three stars are presented in Fig. 2. We show the literature values (blue), derived parameters with $\log g$ fixed to the literature value (green), and derived parameters when $\log g$ is free during the minimization procedure (red points).

5.2. Arcturus

Arcturus is one of the brightest stars on the night sky with a V magnitude of -0.05 (Ducati 2002). Hence it is a prime target for testing with the numerous measurements of the atmospheric parameters as mentioned above.

The atlas consists of both a summer observation set and a winter observation set. The two data sets have been obtained in order to minimise the effect of tellurics at different spectral regions. A comparison between the two sets of measured EWs - both the manual measurements using IRAF and the automatic measurements using ARES - are shown in Fig. 1. The automatic

[1] The solar parameters used were: $T_{\rm eff}$ = 5777 K, $\log g$ = 4.44 dex, [Fe/H] = 0.00 dex, and $\xi_{\rm micro}$ = 1.00 km/s.

Table 2. Results for the three stars with first set of parameters are the literature values as presented in Table. 1, second set of parameters are results with $\log g$ set to the same value during the minimization procedure as found in the literature (fixed), and last set of parameters are with all parameters free during the minimization procedure.

	HD 20010	10 Leo	Arcturus
Literature			
$T_{\rm eff}$ (lit.)	6152 ± 95	4741 ± 60	4247 ± 37
$\log g$ (lit.)	3.96 ± 0.19	2.76 ± 0.17	1.59 ± 0.04
[Fe/H] (lit.)	−0.27 ± 0.06	−0.03 ± 0.02	−0.54 ± 0.04
$\xi_{\rm micro}$ (lit.)	1.17 ± 0.24	1.45 ± 0.08	1.30 ± 0.12
$\log g$ fixed			
$T_{\rm eff}$	6161 ± 164	4761 ± 118	4357 ± 74
$\log g$	3.96 (fixed)	2.76 (fixed)	1.59 (fixed)
[Fe/H]	−0.18 ± 0.11	0.01 ± 0.07	−0.55 ± 0.04
$\xi_{\rm micro}$	1.72 ± 0.44	1.25 ± 0.11	1.55 ± 0.10
All free			
$T_{\rm eff}$	6162 ± 184	4805 ± 98	4439 ± 62
$\log g$	4.08 ± 0.77	2.42 ± 0.61	1.20 ± 0.20
[Fe/H]	−0.18 ± 0.11	−0.01 ± 0.07	−0.58 ± 0.06
$\xi_{\rm micro}$	1.59 ± 0.49	1.23 ± 0.10	1.55 ± 0.10

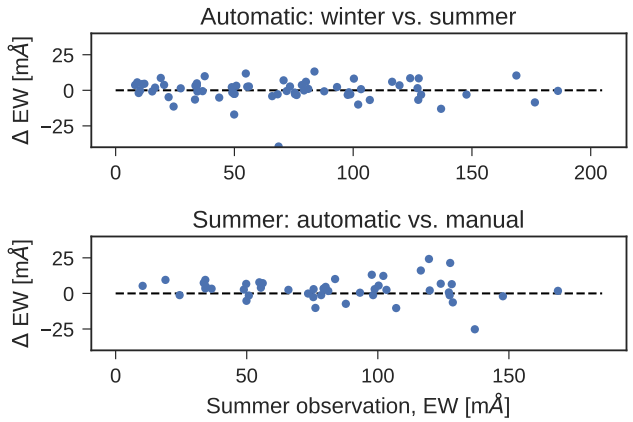

Fig. 1. Top figure: Difference of the automatic EW measurements between the summer observations and winter observations from the Arcturus spectra. Bottom figure: Same as above, but with manual measurements from ARES (summer) and automatic measurements (summer).

EW measurements for the summer set and winter set show excellent agreement with a **mean difference of 3%**. This means that the two data sets are very similar, thus we decided to only manually measure the EWs for one set (summer). We did, however, measure a few lines from the winter data set to verify the agreement. Since the EWs are very similar we chose to only derive parameters of the summer set with EWs measured with ARES.

Due to the low number of pressure sensitive Fe II lines we derive parameters with and without $\log g$ set to a fixed value (1.59 dex, the average literature value adopted). The derivation of the parameters followed the procedure presented in Paper I, although we used the minimization routine of FASMA (Andreasen et al. 2017). After we reached convergence using all the iron lines we were able to measure, one outlier above 3σ in abundance were removed, and the minimization routine was restarted. This process was done iteratively until there were no more outliers. The final results are presented in Table 2 together with mean parameters from the literature.

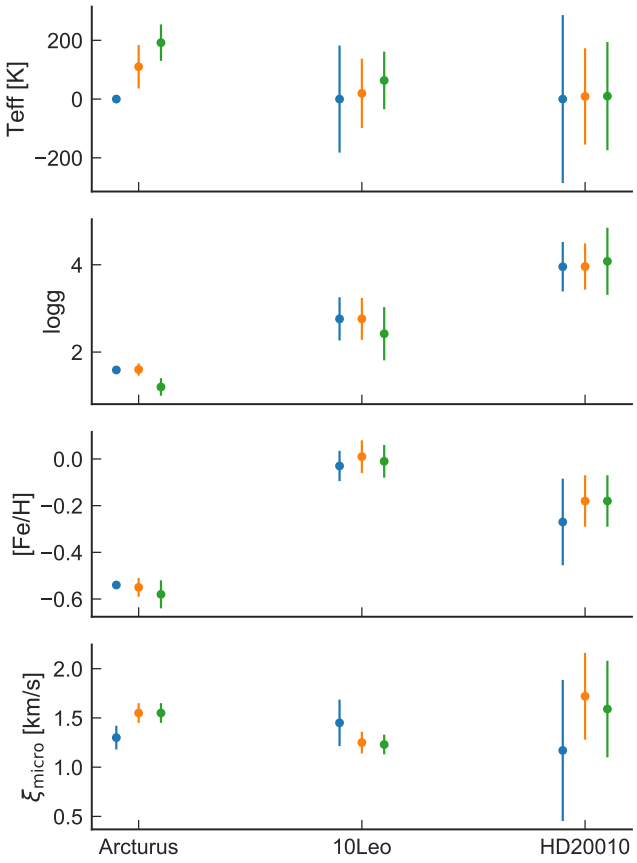

Fig. 2. Parameters for Arcturus, 10 Leo, and HD 20010 (revisited in this paper). The blue points show the literature values as discussed in the text. The green points are the derived values with $\log g$ fixed to the literature value, and the red points show the derived parameters when $\log g$ is also derived. **For $T_{\rm eff}$ the results are shown compared to the literature value to see the difference.**

We derive $T_{\rm eff}$ a 100 K too high for $\log g$ fixed compared to the literature, which is just wihtin the errorbars of the two measurements. When $\log g$ is derived we see a 200 K difference. This especially shows the importance of $\log g$ which we derive 0.4 dex lower than the literature value. The metallicity is derived with rather high precision (0.04 dex) when $\log g$ is fixed and 0.10 dex when it is derived. The value in both cases are well within the errors of the literature value.

5.3. 10 Leo

The approach for determining the atmospheric stellar parameters for 10 Leo is identical to Arcturus. We use ARES on each band (YJ, H, and K-band) separately. For the small gaps in the spectrum, we simply set the flux to 1, since the spectrum is already normalised. This will also prevent ARES to identify and measure any lines in these regions. The EWs from the three regions are combined to one final line list used for the determination of the parameters. The final results can be seen in Fig. 2 and Table 2.

Generally the derived parameters are in excellent agreement with the literature values listed here. For $T_{\rm eff}$ we were 64 K off with $\log g$ set as a free parameter, well within the errors. The only parameter that show a discrepancy compared to the literature value is $\xi_{\rm micro}$ with a difference of 0.22 km/s, which is at the limit of the errors reported. We note that this parameter is not

reported in the PASTEL database, and this was a derived parameter from a empirical relation. We were able to derive good $\log g$ values, although with larger errors compared to the results from the literature.

6. Discussion

6.1. The role of $\log g$

One of the most difficult atmospheric stellar parameters to get from a spectrum is the surface gravity. For this we need the lines of pressure sensitive ionized atoms such as Fe II. However, they are more sparse than neutral iron, Fe I, making the determination more challenging. This is true in the optical (see e.g. the discussion by Mortier et al. 2013), and even more in the NIR (see e.g. Paper I). One solution to this problem is to fix the value of surface gravity and derive the other parameters. With the parallaxes from e.g. Gaia (Gaia Collaboration et al. 2016) we will have access to accurate $\log g$. However, this requires a priori knowledge of the mass from e.g. isochrones, and $T_{\rm eff}$. By iteratively obtaining the $T_{\rm eff}$ from spectroscopy and the corresponding $\log g$ from the parallaxes, we can obtain reliable $T_{\rm eff}$, $\log g$, and [Fe/H]. Another approach is to use asteroseismic $\log g$ which are becoming a new standard. This has previously been done in the APOGEE+*Kepler* (APOKASC) context by Pinsonneault et al. (2014); Hawkins et al. (2016). It is important to mention, that the asteroseismic $\log g$ in turn is dependent on $T_{\rm eff}$ through the scaling relations (see e.g. Kjeldsen & Bedding 1995). Moreover, this is not possible for all spectral classes. It is e.g. not possible for M dwarfs, since no pulsations have been observed here.

Since there is a dependence between the other derived parameters with $\log g$, simply using a mean value as a reference value can lead to misleading parameters. To verify the impact of using the wrong $\log g$ as baseline, we tested what was the $T_{\rm eff}$ and [Fe/H] that we derive by setting $\log g$ fixed to values between 0.9 dex and 2.2 dex, i.e., in the range of the literature values found. The results show that $T_{\rm eff}$ and [Fe/H] can change by 200 K and 0.21 dex, respectively. This is most likely the origin of the small discrepancies seen for the parameters of Arcturus when the $\log g$ is fixed and free.

Furthermore, note that the ionized iron lines are not only sparse, they are also rather weak. The lowest measured EW for an Fe II line is 9.7 mÅ (in Arcturus), while the highest measured value is 24.4 mÅ (in 10 Leo). However, with the upcoming high quality spectra for the NIR, the community should still be able to measure these Fe II lines. We showed in Paper I that a minimum S/N of around 50 is required to utilise this method, however this was only tested for the Sun, and a higher S/N might be needed for other spectral types.

6.2. Proper data reduction

The relative novelty of NIR high resolution spectroscopy is reflected on a number of problems regarding the available spectra that made our analysis particularly difficult. For instance, in Paper I we had to deal with a less reliable wavelength calibration for the spectrum of HD 20010. This meant the wavelength was stretched when compared to a synthetic spectrum, which is discussed in more detail by Nicholls et al. (2017). The poor wavelength calibration for HD 20010 most likely caused bad EW measurements. In addition, the spectrum was not corrected for telluric lines which also caused minor deviation from the true EW when measured. Another reason was the non-refined line list used, which we have attempted to correct for here. The refined line list has made the derivation of the metallicity more reliable compared with the adopted literature as it is demonstrated in Sec. 5.1. It is expected that even better results will be obtained for this star once the final spectrum is presented by the CRIRES-POP team.

All the above problems we had with HD 20010 have been solved for 10 Leo, and it is clear the results are of much higher quality. This can be seen by the smaller errors we have on our parameters, and the good agreement of all parameters compared with the literature. Therefore, it may be necessary that a telluric correction is applied to the spectrum before atmospheric stellar parameters can be determined reliably. However, with our limited sample it is difficult to make a clear conclusion yet. Note that this is unlike the optical where a telluric correction is not necessary for obtaining atmospheric parameters.

6.3. The refined line list

The line list from Paper I has been refined, i.e. several blended or otherwise unreliable measured lines have been removed. This was done using the same solar spectrum as in Paper I. In order to test this new line list it was first used to re-derive parameters for HD 20010, which was the test case in Paper I. Using the refined line list we were able to reduce the error, and derive parameters closer to the literature values. Especially important is the derived metallicity which was previously over-estimated by $\sim$ 0.1 dex. With the refined line list the metallicity went from -0.14 ± 0.14 dex to -0.18 ± 0.11, showing an overall improvement.

Furthermore, the refined line list was tested on the two K giants, Arcturus and 10 Leo. We see a good agreement between the derived parameters and the literature values used for comparison **as discussed above in the text. Additionally we mark two lines as outliers in Table A.1, which were both removed during the derivation of stellar parameters for both stars. These lines are the two Fe I lines at** 10 167.47 Å **and** 11 641.80 Å**.**

While this line list, and in particular this method for obtaining stellar atmospheric parameters, will fail at higher $T_{\rm eff}$, (above $\sim$ 7000 K[2]) it should still work at lower $T_{\rm eff}$. The biggest challenge in this regime is the continuum depression by molecular lines, however this is a smaller effect compared with the optical part of the spectrum. Hence it will still be interesting to see how far this line list might work in terms of $T_{\rm eff}$.

7. Conclusion

In this paper we presented a refined Fe I and Fe II line list in the NIR domain to derive parameters for high resolution spectra. The method should work in all spectral ranges, however, it is important to locate the appropriate iron lines. For the NIR we need a relative large coverage (YJHK, although few lines are in the K band). The method used here which is usually adopted in the optical domain to derive parameters is now available for the NIR as well. The refined line list has been used to derive new parameters for the late F-star HD 20010, as well as for two K-giants (Arcturus and 10 Leo). The results show that the stellar atmospheric parameters derived using our line list are perfectly compatible with the literature values. We are thus now extending the line list towards cooler temperatures. With the updated results for HD 20010, and the results for Arcturus and 10 Leo, we are now reaching the same precision that has been reached

[2] Due to the low number of absorption lines and non-LTE effects.

in the optical for similar spectral types using the same methodology. The obvious next step is to approach the even cooler M stars. Particular interesting are the M dwarf stars, known to be prone forming rocky planets. As important as cooler stars, we have yet to test our line list on any dwarf stars other than the Sun for which our line list is calibrated. The upcoming spectral library from CARMENES (priv. comm. with P. Amado) will provide the community with high quality spectra and allow us to extend our test to many different spectral types of interest.

Acknowledgements. We thank José Caballero for many useful comments during the process which led to this paper. This work was supported by Fundação para a Ciência e a Tecnologia, FCT, (ref. UID/FIS/04434/2013, PTDC/FIS-AST/1526/2014, and PTDC/FIS-AST/7073/2014) through national funds and by FEDER through COMPETE2020 (ref. POCI-01-0145-FEDER-007672, POCI-01-0145-FEDER-016886, and POCI-01-0145-FEDER-016880). N.C.S., and S.G.S. acknowledge the support from FCT through Investigador FCT contracts of reference IF/00169/2012, and IF/00028/2014, respectively, and POPH/FSE (EC) by FEDER funding through the program "Programa Operacional de Factores de Competitividade - COMPETE". E.D.M acknowledge the support from the FCT in the form of the grants IF/00849/2015/CP1273/CT0003. JJN acknowledges support from FCT in the form of a "PhD::Space" (PD/00040/2012) network doctoral grant, of reference PD/BD/52700/2014. This research has made use of the SIMBAD database operated at CDS, Strasbourg (France).

References

Adibekyan, V. Z., Benamati, L., Santos, N. C., et al. 2015, MNRAS, 450, 1900
Ammler-von Eiff, M., Santos, N. C., Sousa, S. G., et al. 2009, A&A, 507, 523
Andreasen, D. T., Sousa, S. G., Delgado Mena, E., et al. 2016, A&A, 585, A143
Andreasen, D. T., Sousa, S. G., Tsantaki, M., et al. 2017, A&A, 600, A69
Baraffe, I., Homeier, D., Allard, F., & Chabrier, G. 2015, A&A, 577, A42
Bensby, T., Feltzing, S., & Oey, M. S. 2014, A&A, 562, A71
Berdiñas, Z. M., Rodríguez-López, C., Amado, P. J., et al. 2017, MNRAS, 469, 4268
Bertaux, J. L., Lallement, R., Ferron, S., Boonne, C., & Bodichon, R. 2014, A&A, 564, A46
Blackwell, D. E. & Shallis, M. J. 1977, MNRAS, 180, 177
Boyajian, T. S., von Braun, K., van Belle, G., et al. 2012, ApJ, 757, 112
Casagrande, L., Ramírez, I., Meléndez, J., Bessell, M., & Asplund, M. 2010, A&A, 512, A54
Dotter, A., Chaboyer, B., Jevremović, D., et al. 2008, ApJS, 178, 89
Ducati, J. R. 2002, VizieR Online Data Catalog, 2237
Gaia Collaboration, Prusti, T., de Bruijne, J. H. J., et al. 2016, A&A, 595, A1
Girardi, L., Bressan, A., Bertelli, G., & Chiosi, C. 2000, A&A Supp., 141, 371
Gonzalez, G. & Laws, C. 2000, AJ, 119, 390
Griffin, R. & Griffin, R. 1967, MNRAS, 137, 253
Hawkins, K., Masseron, T., Jofré, P., et al. 2016, A&A, 594, A43
Hinkle, K., Wallace, L., & Livingston, W. 1995a, PASP, 107, 1042
Hinkle, K. H., Wallace, L., & Livingston, W. 1995b, in Astronomical Society of the Pacific Conference Series, Vol. 81, Laboratory and Astronomical High Resolution Spectra, ed. A. J. Sauval, R. Blomme, & N. Grevesse, 66
Jofré, P., Heiter, U., Soubiran, C., et al. 2014, A&A, 564, A133
Kjeldsen, H. & Bedding, T. R. 1995, A&A, 293, 87
Kupka, F. G., Ryabchikova, T. A., Piskunov, N. E., Stempels, H. C., & Weiss, W. W. 2000, Baltic Astronomy, 9, 590
Kurucz, R. 1993, ATLAS9 Stellar Atmosphere Programs and 2 km/s grid. Kurucz CD-ROM No. 13. Cambridge, Mass.: Smithsonian Astrophysical Observatory, 1993., 13
Lebzelter, T., Heiter, U., Abia, C., et al. 2012a, A&A, 547, A108
Lebzelter, T., Seifahrt, A., Uttenthaler, S., et al. 2012b, A&A, 539, A109
Lindgren, S., Heiter, U., & Seifahrt, A. 2016, A&A, 586, A100
McWilliam, A. 1990, ApJS, 74, 1075
Meléndez, J. & Barbuy, B. 1999, ApJS, 124, 527
Mortier, A., Santos, N. C., Sousa, S. G., et al. 2013, A&A, 558, A106
Mucciarelli, A., Pancino, E., Lovisi, L., Ferraro, F. R., & Lapenna, E. 2013, ApJ, 766, 78
Nicholls, C. P., Lebzelter, T., Smette, A., et al. 2017, A&A, 598, A79
Önehag, A., Heiter, U., Gustafsson, B., et al. 2012, A&A, 542, A33
Pinsonneault, M. H., Elsworth, Y., Epstein, C., et al. 2014, ApJS, 215, 19
Piskunov, N. E., Kupka, F., Ryabchikova, T. A., Weiss, W. W., & Jeffery, C. S. 1995, A&A Supp., 112, 525
Ramírez, I., Allende Prieto, C., & Lambert, D. L. 2013, ApJ, 764, 78
Ramírez, I. & Meléndez, J. 2005, ApJ, 626, 446
Recio-Blanco, A., Bijaoui, A., & de Laverny, P. 2006, MNRAS, 370, 141
Rodríguez, E., Rodríguez-López, C., López-González, M. J., et al. 2016, MNRAS, 457, 1851
Santos, N. C., Sousa, S. G., Mortier, A., et al. 2013, A&A, 556, A150
Smiljanic, R., Korn, A. J., Bergemann, M., et al. 2014, A&A, 570, A122
Sneden, C. A. 1973, PhD thesis, THE UNIVERSITY OF TEXAS AT AUSTIN.
Soubiran, C., Le Campion, J.-F., Brouillet, N., & Chemin, L. 2016, A&A, 591, A118
Sousa, S. G., Santos, N. C., Adibekyan, V., Delgado-Mena, E., & Israelian, G. 2015, A&A, 577, A67
Sousa, S. G., Santos, N. C., Mayor, M., et al. 2008, A&A, 487, 373
Torres, G., Andersen, J., & Giménez, A. 2010, A&A Rev., 18, 67
Torres, G., Fischer, D. A., Sozzetti, A., et al. 2012, ApJ, 757, 161
Torres, G., Winn, J. N., & Holman, M. J. 2008, ApJ, 677, 1324
Tsantaki, M., Andreasen, D. T., Teixeira, G. D. C., et al. 2017, MNRAS, 555, A150
Tsantaki, M., Sousa, S. G., Adibekyan, V. Z., et al. 2013, A&A, 555, A150
Valenti, J. A. & Fischer, D. A. 2005, ApJS, 159, 141
Worley, C. C., de Laverny, P., Recio-Blanco, A., Hill, V., & Bijaoui, A. 2016, A&A, 591, A81

Appendix A: Complete refined line list

The complete refined line list with Solar EWs measured by hand using IRAF, and the three stars also analysed in this work. Note that the EWs given here are after removal of outliers in abundance. This is done automatically with FASMA (Andreasen et al. 2017).

Table A.1. Refined line list with all Fe I and Fe II lines and corresponding atomic data, including the updated log *gf*. The fifth to the eight columns are the measured EWs in mÅ for the four stars analysed in this work. **The last column shows where Arcturus and 10 Leo both had outliers in the derivation of parameters.** This table is available in an electronic form online.

Wavelength (Å)	Element	EP (eV)	log *gf*	Sun	HD 20010	10 Leo	Arcturus	Giant outlier
10065.05	Fe I	4.83	-0.279	94.0	...	115.2	107.0	no
10080.42	Fe I	5.10	-1.964	5.9	...	...	...	no
10081.39	Fe I	2.42	-4.512	6.9	...	42.9	49.8	no
10086.24	Fe I	2.95	-3.978	7.0	39.5	34.2	...	no
10137.10	Fe I	5.09	-1.736	9.8	...	21.1	12.1	no
10142.84	Fe I	5.06	-1.554	14.9	5.5	36.3	...	no
10145.56	Fe I	4.80	-0.118	109.0	146.5	137.0	...	no
10155.16	Fe I	2.18	-4.336	16.2	79.0	87.8	...	no
10156.51	Fe I	4.59	-2.109	12.2	...	29.2	24.4	no
10167.47	Fe I	2.20	-2.319	125.7	...	...	...	yes
10195.11	Fe I	2.73	-3.608	22.6	10.7	76.3	78.4	no
10216.31	Fe I	4.73	0.047	129.9	144.9	128.6	...	no
10218.41	Fe I	3.07	-2.893	40.9	101.7	98.2	...	no
10265.22	Fe I	2.22	-4.648	8.1	...	52.6	55.4	no
10307.45	Fe I	4.59	-2.432	6.4	16.8	9.1	...	no
10332.33	Fe I	3.63	-3.131	10.5	...	48.6	34.4	no
10340.89	Fe I	2.20	-3.665	46.6	116.5	127.1	...	no
10347.97	Fe I	5.39	-0.717	37.0	19.5	58.2	36.6	no
10353.81	Fe I	5.39	-0.989	24.2	12.1	39.6	33.4	no
10364.06	Fe I	5.45	-1.100	18.0	9.0	33.5	16.6	no
10379.00	Fe I	2.22	-4.236	18.7	6.2	76.4	80.1	no
10388.75	Fe I	5.45	-1.471	8.7	...	16.5	8.2	no
10395.80	Fe I	2.18	-3.435	61.3	129.3	147.7	...	no
10423.03	Fe I	2.69	-3.658	22.9	8.4	80.6	79.3	no
10423.74	Fe I	3.07	-3.119	29.9	...	...	...	no
10469.65	Fe I	3.88	-1.277	89.3	131.9	127.4	...	no
10532.24	Fe I	3.93	-1.650	64.4	109.1	98.8	...	no
10555.65	Fe I	5.45	-1.282	13.1	7.1	25.5	15.4	no
10577.14	Fe I	3.30	-3.222	17.2	6.0	67.0	56.1	no
10616.72	Fe I	3.27	-3.306	15.6	6.5	57.0	50.8	no
10725.19	Fe I	3.64	-2.948	15.7	6.8	57.5	48.9	no
10753.00	Fe I	3.96	-2.077	39.7	81.8	73.4	...	no
10780.69	Fe I	3.24	-3.553	10.4	...	49.7	34.2	no
10783.05	Fe I	3.11	-2.786	47.0	100.4	103.3	...	no
10818.28	Fe I	3.96	-2.160	35.6	20.3	76.2	...	no
10863.52	Fe I	4.73	-0.877	67.1	84.2	75.4	...	no
10884.26	Fe I	3.93	-2.129	39.1	79.3	75.5	...	no
10896.30	Fe I	3.07	-2.911	42.9	101.8	100.3	...	no
11013.24	Fe I	4.80	-1.240	42.4	...	...	...	no
11026.79	Fe I	3.94	-2.517	21.2	49.4	68.6	...	no
11119.80	Fe I	2.85	-2.452	84.8	142.5	...	...	no
11641.80	Fe I	4.58	-2.116	15.6	...	...	...	yes
11778.42	Fe I	5.34	-1.708	8.4	6.3	11.2	...	no
12053.08	Fe I	4.56	-1.602	41.3	33.5	76.5	...	no
12119.50	Fe I	4.59	-1.897	25.0	...	50.1	...	no
12213.34	Fe I	4.64	-2.006	19.1	16.5	37.5	...	no
12227.11	Fe I	4.61	-1.408	51.5	...	72.0	...	no
12244.92	Fe I	3.64	-3.222	11.8	54.2	...	...	no
12340.48	Fe I	2.28	-4.680	9.4	...	58.2	54.8	no
12342.92	Fe I	4.64	-1.545	42.1	19.4	80.4	65.9	no
12510.52	Fe I	4.96	-1.930	12.9	39.1	20.4	...	no
12557.00	Fe I	2.28	-4.026	33.8	14.6	113.7	124.0	no
12615.93	Fe I	4.64	-1.686	35.7	...	44.1	...	no
12638.70	Fe I	4.56	-0.679	112.3	...	...	...	no
12807.15	Fe I	3.64	-2.649	37.1	...	97.7	...	no
12808.24	Fe I	4.99	-1.811	16.4	9.8	47.9	33.6	no
12824.86	Fe I	3.02	-3.612	20.1	6.6	84.1	83.7	no

Table A.1. continued.

Wavelength (Å)	Element	EP (eV)	log *gf*	Sun	HD 20010	10 Leo	Arcturus	Giant outlier
12840.57	Fe I	4.96	-1.612	25.3	10.9	72.1	...	no
12879.77	Fe I	2.28	-3.525	68.7	126.2	168.7	...	no
12896.12	Fe I	4.91	-1.713	23.2	12.4	55.7	49.1	no
12933.01	Fe I	5.02	-1.879	13.9	6.6	19.0	...	no
12934.67	Fe I	5.39	-1.103	30.9	20.8	49.9	...	no
13014.84	Fe I	5.45	-1.542	12.3	10.4	22.3	...	no
13352.17	Fe I	5.31	-0.355	94.4	74.8	145.3	...	no
13392.10	Fe I	5.35	-0.105	115.1	142.4	...	...	no
15194.49	Fe I	2.22	-4.808	14.1	...	116.4	...	no
15201.57	Fe I	5.49	-1.315	29.0	...	43.6	...	no
15490.34	Fe I	2.20	-4.787	16.1	...	70.3	119.5	no
15593.74	Fe I	5.03	-1.796	28.0	14.6	65.5	...	no
15611.15	Fe I	3.42	-2.966	51.6	31.4	102.1	...	no
15648.51	Fe I	5.43	-0.633	93.8	57.2	138.5	127.6	no
15676.58	Fe I	5.11	-1.848	22.3	36.1	27.4	...	no
16198.50	Fe I	5.41	-0.376	131.4	84.7	172.3	176.5	no
17420.83	Fe I	3.88	-3.628	6.7	51.0	...	...	no
19923.34	Fe I	5.02	-1.536	49.7	128.6	119.8	...	no
21851.38	Fe I	3.64	-3.578	12.7	5.0	62.5	...	no
22257.11	Fe I	5.06	-0.704	132.5	109.3	...	...	no
22380.80	Fe I	5.03	-0.377	179.4	107.8	...	...	no
22392.88	Fe I	5.10	-1.330	60.8	32.9	171.8	128.2	no
22619.84	Fe I	4.99	-0.564	158.2	...	...	...	no
23308.48	Fe I	4.08	-2.705	31.3	80.9	68.2	...	no
10427.31	Fe II	6.08	-1.575	13.7	8.1	20.7	10.3	no
10501.50	Fe II	5.55	-1.861	19.5	16.8	24.4	...	no
10862.64	Fe II	5.59	-2.006	15.3	15.8	10.0	9.7	no
11125.58	Fe II	5.62	-2.213	10.5	14.1	...	...	no
13251.14	Fe II	9.41	0.768	13.4	50.3	...	...	no